Sun *et al.*
BMC Complementary Medicine and Therapies (2023) 23:60
https://doi.org/10.1186/s12906-023-03883-3

BMC Complementary Medicine and Therapies

RESEARCH

Open Access

A multi-target protective effect of Danggui-Shaoyao-San on the vascular endothelium of atherosclerotic mice

Yuemeng Sun, Yushan Gao, Lu Zhou, Yixing Lu, Yulin Zong, Haoyu Zhu, Yang Tang, Fengjie Zheng, Yan Sun* and Yuhang Li*

Abstract

Background Atherosclerosis (AS) is a chronic disease characterized by abnormal blood lipid metabolism, inflammation and vascular endothelial injury. Vascular endothelial injury is the initial stage during the occurrence of AS. However, the function and mechanism of anti-AS are not well characterized. Danggui-Shaoyao-San (DGSY) is a classic Traditional Chinese Medicine (TCM) prescription for the treatment of gynecological diseases, and has been widely used in the treatment of AS in recent years.

Methods ApoE$^{-/-}$ atherosclerosis male mice were established by feeding with high-fat diet, and then randomly divided into three groups: Atherosclerosis group (AS), Danggui-Shaoyao-San group (DGSY), and Atorvastatin calcium group (X). The mice were administered with the drugs for 16 weeks. Pathological changes in aortic vessels were examined by staining with Oil red O, Masson and hematoxylin–eosin. In addition, blood lipids were analyzed. The level of IL-6 and IL-8 in aortic vessels were detected by ELISA and the expression of ICAM-1 and VCAM-1 in the aortic vascular endothelium were measured by Immunohistochemical. The mRNA expression of interα5β1/c-Abl/YAP in the aortic vessels were measured by Real-time quantitative PCR and location of expression was assessed by immunofluorescence.

Results DGSY can significantly reduce the content of TC,TG and LDL-C and increase the level of HDL-C in the serum, reduce the plaque area and inhibit the concentration of IL-6 and IL-8, down-regulate the expression of IVAM-1,VCAM-1 and interα5β1/ c-Abl/YAP in the aortic vessels.

Conclusions Collectively, DGSY can alleviate vascular endothelium damage and delay the occurrence of AS, and the underlying mechanism may be related to the multi-target protective of DGSY.

Keywords Danggui-Shaoyao-San, Atherosclerosis, Vascular endothelium, Multiple targets, Interα5β1/c-Abl/YAP

Introduction

Atherosclerosis (AS), as a pathological basis of cardiovascular and cerebrovascular diseases, is the main cause of ischemic heart disease and stroke [1]. It is characterized by abnormal lipid metabolism, inflammatory reactions, vascular endothelial dysfunction, and plaque formation [2]. Globally, almost 20 million people die from AS-related diseases every year making it a serious threat to human health. In Europe, four million

*Correspondence:
Yan Sun
suny@bucm.edu.cn
Yuhang Li
liyuhang@bucm.edu.cn
School of Chinese Medicine, Beijing University of Chinese Medicine, Beijing 100029, China

people die from cardiovascular diseases every year [3]. Moreover, AS reduces the quality of life of patients, creating challenges for their immediate society [4, 5]. Therefore, it is imperative to either prevent or delay AS progression. Although the pathogenesis of AS is not well understood, vascular endothelial dysfunction has been linked to the occurrence of AS [6]. Endothelial barrier dysfunction leads to lipid deposition in the vascular wall and the invasion of inflammatory cells [7], resulting in plaque formation. Therefore, protection of the vascular endothelium is an effective method to prevent or treat AS.

Danggui-Shaoyao-San (DGSY) is a classic prescription of traditional Chinese medicine. DGSY is composed of six medicinal herbs — Danggui (*Angelica Sinensis Ridix*), Baishao (*Paeoniae Radix Alba)*, Fuling (*Poria*), Chuanxiong (*Chuanxiong Rhizoma*), Zexie (*Alismatis Rhizoma*) and Baizhu (*Atractylodis Macrocephalae Rhizoma*) — in the ratio 9:48:12:24:24:12. DGSY has recently been used in the treatment of AS [8–11]. Moreover, DGSY reduced total cholesterol (TC), triglyceride (TG), and low-density lipoprotein (LDL), and increased high-density lipoprotein (HDL) in gestational hypertension murine models [12]. Similarly, DGSY reduced blood viscosity and red blood cell aggregation in rabbits; improved hemorheology abnormalities; reduced the expression of AngII and AT1R in podocytes from rats with nephrotic syndrome; improved proteinuria [13, 14] as well as downregulated the specific expression of vascular adhesion molecule 1 (VCAM-1) mRNA in dyslipidemia; exhibited antimonocyte adhesion; and protected vascular endothelial function [15]. Furthermore, ferulic, paeoniflorin, and poria acids, the active ingredients in DGSY, inhibited the secretion of IL-6 and TNF-α, and reduced cellular inflammation [16]. Although numerous experimental studies have provided a pharmacological basis for the treatment of AS with DGSY, its detailed mechanism of action is yet to be fully elucidated. Despite the various drugs for the treatment of AS, their side effects limit their clinical application [17, 18]. Conversely, traditional Chinese herbal medicines like DGSY are characterized by few side effects and low toxicity [19–21], probably resulting in the recent interest in their use for the treatment of AS.

In the present study, we determined the multi-target protective effect of DGSY on vascular endothelium in an AS murine model. Specifically, we determined its regulatory effect on the interα5β1/c-Abl/YAP turbulence signal associated with vascular endothelial dysfunction to reveal potential mechanisms of AS. This study establishes the clinical application of DGSY for the treatment of vascular endothelial damage and the prevention of AS.

Materials and methods

Animal rearing and treatment

Mice were reared independently in ventilation cage systems of the animal room of the Beijing University of Chinese Medicine at 25(±2) ℃ and relative humidity of 40%-60% under a 12-h day and 12-h night cycle. Both food and water were freely availed to the mice. All experimental protocols were approved by the Animal Ethics Committee of Beijing University of Chinese Medicine (Approval Batch No: BUCM-4–2021060802-2056). After adaptive feeding for a week, ApoE-/- mice were randomly divided into three groups (n 1/3 12 each): Model group (M), Danggui-Shaoyao-San group (DGSY), and Atorvastatin calcium group (X). All were fed a high-fat diet (15% lard, 2% cholesterol, and 0.05% cholic acid) from Beijing Vital River Laboratory Animal Technology. Twelve C57BL/6 J mice served as the normal control group (NC) and were fed a conventional diet throughout the experimental period. Mice were continuously fed for 16 weeks to establish the AS model. In the first week of the experiment, the DGSY group was administered a 16.77 g/kg/d dose of DGSY intragastrically, and the X group was given a 5 mg/kg/d dose of atorvastatin calcium tablets (H20051408, New York, United States) intragastrically. The NC and the AS groups were given a similar dose of distilled water intragastrically. After treatment for 16 weeks, the mice were sacrificed via overdoses of sodium pentobarbital. Blood samples were obtained, six aortic vessels were dissected, fixed with 4% paraformaldehyde, and stored at 4℃ (BCD-315TNGS, Qingdao, China) for subsequent experimentations. Moreover, six aortic vessels from each group were stored at -80℃ (ULTS1490, Suzhou, China).

Preparation of drugs

Atorvastatin calcium tablets were ground into powder and dissolved in distilled water when required.

DGSY was purchased from Beijing Tong Ren Tang Jingxi Pharmacy Co., LTD (Beijing, China) and is shown in Fig. 1. The crude herbs constituted with six herbs[10]and their proportions were shown in Table 1.

These herbs were first placed in an AI electric earthenware pot (GX-500A, Guangdong, China) and soaked for 30 min in distilled water, before boiling at medium heat for 30 min to obtain the decoction which was then decanted. Subsequently, 1000 ml water was added to the herbs and the process was repeated. The two drug decoctions were mixed and concentrated to 2 g/ml and then stored at 4℃.

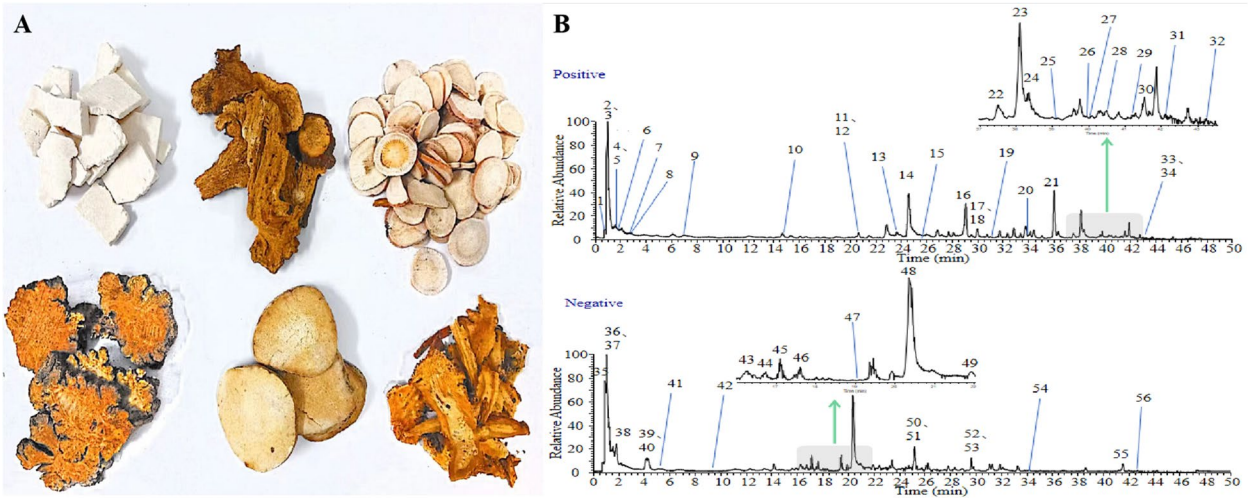

Fig. 1 **A** Herbal composition of DGSY. **B** Total ion chromatogram of DGSY

Table 1 Compositions of medicinal herbs in DSGY

Name of medicine herbs	DGSY(g)
Angelica Sinensis Ridix	9
Paeoniae Radix Alba	48
Poria	12
Chuanxiong Rhizoma	24
Alismatis Rhizoma	24
Atractylodis Macrocephalae Rhizoma	12

Ultra-high performance liquid chromatography-mass spectrometry analysis (UHPLC-MS)

The DGSY solution was extracted in methanol, and the supernatant was filtered through 0.22 μm microporous membranes. This was injected into a UHPLC-LTQ-Orbitrap-MS system.

Oil red O Staining

Frozen aortic vessels were cut into 10 μm slices (CM 1950, Leica, Germany), air-dried, then stained with Oil Red O (G1261, Solarbio, China) according to the manufacturer's instructions. To evaluate the effect of drug administration, the ORO-stained slides were observed and recorded under a positive fluorescence microscope (DM4B, Leica, Germany) (100x), then marked and assessed with Image-Pro Plus version 6.0 analysis software (Media Cybernetics, Maryland, United States).

Masson's trichrome staining

Frozen aortic vessel slides were air-dried and then stained with Masson's trichrome dye (G1345, Solarbio, China) according to the manufacturer's instructions. The vascular morphological changes were observed and recorded under a positive fluorescence microscope (100x, 200x).

Hematoxylin and eosin staining

Frozen aortic vessel slides were obtained from each group and dried on a bench and then stained with hematoxylin and eosin (HE, KIT-9706, MXB, Fujian, China). Morphological changes in aortic vessels were observed and recorded under a positive fluorescence microscope (100x, 200x).

Measurements for serum biochemical markers

Retro-orbital bleeding was collected into 1.5 ml centrifuge tubes and stored at 4℃ for 4 h. Samples were then centrifuged (3000 rpm, 10 min) and the supernatants were collected. In these, the levels of TC, TG, LDL-C, and HDL-C were measured by a vertical automatic blood biochemical analyzer (7080, HITACHI, Shanghai, China).

ELISA analysis

Aortic vessel tissue samples were ground with a high throughput cryogenic tissue grinder (Scientz-48L, Ningbo, China) to obtain homogenates which were then centrifuged at 12000 rpm for 15 min at 4℃ (Eppendorf 5425 R, Hamburg, Germany). IL-6 (1203210413, RayBio, Atlanta, United States) and IL-8 (M211224-104a, Neobioscience, Shenzhen, China) were assayed according to the manufacturer's instructions, and the absorbance was measured at 450 nm.

Immunohistochemical analysis

Frozen aortic vessel slides were incubated at 95 °C for 10 min in sodium citrate for thermal antigen repair,

before rinsing thrice with PBS —each time for 5 min— and incubating with goat serum for 10 min. Slides were then incubated with the primary antibody (intercellular adhesion molecule 1 (ICAM-1) (1:280); VCAM-1 (1:50) at 4℃ overnight. Then the slides were incubated with a secondary antibody for 1 h and visualized with DAB (2109290031H, MXB, Fujian, China). The sections were observed under a positive fluorescence microscope to assess the loci of positive expression and the depth of staining. Positive expression was denoted by either yellow or brownish-yellow stained particles. The sections were recorded with Image-Pro Plus version 6.0 analysis software.

Real-time quantitative PCR analysis

Total RNA was extracted from aortic vessels using Trizol (15,596,018, Invitrogen, California, United States) using the reverse transcription kit (K1622, Thermo, Massachusetts, United States) in line with the manufacturer's instructions. The concentration and purity were measured and samples were reverse-transcribed to cDNA. The PCR primers targeting *interα5β*, *c-Ab1*, *YAP*, and *GAPDH* genes are shown in Table 2. The PCR cycling conditions were: one cycle at 95 °C for 5 min, then 40 cycles for 95 °C for 15 s, 60 °C for 20 s, and 72 °C for 30 s. The relative expression of target genes was calculated by $2^{-\Delta\Delta CT}$.

Immunofluorescence staining

Frozen aortic vessel slides were incubated in sodium citrate at 95 °C for 10 min for thermal antigen repair. interα5β1(1:100), c-Abl (1:50), and YAP (1:50) were used as primary antibodies and goat anti-rabbit IgG was used as the secondary antibody. After reactions with the primary antibodies, samples were incubated overnight at 4℃ before the fluorescent secondary antibody was added. Both samples were diluted with PBS (1:200) followed by incubation for 1 h. Then, a drop of anti-fluorescence quencher containing DAPI (GR3405163-3, Abcam, Cambridge, United Kingdom) was added to cover the glass seal. The sections were observed under a positive fluorescence microscope.

Table 2 Primer sequences used for qPCR

genes	Forward Primer (5′-3′)	Reverse Primer (5′-3′)
Inter α5β1	GGCTATGTCACCGTCCTTAAT	CTAGCCCATCTCCATTGGTATC
YAP	GAAAGGGCTCTAGTGGGT AAAG	AAATCAGGCTAAGGGAAG TAAGG
c-Ab1	GGAGTATTGCTCTGGGAG ATTG	GCTCCATGCGGTAGTCTTT
GAPDH	AACAGCAACTCCCACTCTTC	CCTGTTGCTGTAGCCGTATT

Data analysis

SPSS software v.22 was used for statistical analysis. All data were expressed as mean ± standard deviation (SD). One-way ANOVA was used to compare multiple groups. The LSD method was used to compare the differences between the groups when the variance was homogeneous. The Games-Howell method was used to compare differences between groups when the variance was not uniform. A value of $p < 0.05$ indicated that the difference was statistically significant.

Results

DGSY Components

DGSY samples were analyzed after chromatographic separation due to the optimized LC–ESI–MS method. There were 56 peaks in chromatograms of DGSY samples, which consisted of ferulic acid, ligustrolide, paeoniflorin, and other compounds as shown in Fig. 1 and Table 3.

Effects of DGSY on pathological morphology of aortic vessels

To observe the effect of DGSY on the morphology of aortic vessels, Oil red O, Masson, and HE stained slides were analyzed (Fig. 2). Compared with the NC group, the pathological morphology of the murine aortic vessels in the AS group had different degrees of injury. Oil red O stains showed that the aortic plaque area had significantly increased whereas Masson stains showed a decrease in aortic collagen fibers. HE staining showing significant intimal thickening of the aortic wall, disordered arrangement of endothelial cells, increased lipid deposition, and pronounced plaque protrusion into the lumen. After 16 weeks of drug intervention (Fig. 2B & C), aortic plaques were significantly reduced and aortic collagen fibers were significantly increased in DGSY and X groups. The improvement of vascular pathological morphology in the DGSY was higher compared with that of X group, indicating that DGSY effectively prevented atherosclerosis.

Effects of DGSY on disordered lipid metabolism

To determine the regulatory effect of DGSY on blood lipid metabolism, TC, TG, LDL-C, and HDL-C levels in the serum of mice were quantified. Levels of TC, TG, and LDL-C in serum were significantly higher ($P < 0.01$) in the M than NC group. Conversely, the levels of HDL-C were lower ($P < 0.01$) (Fig. 3). This indicated that the high-fat diet induced AS mice had typical dyslipidemia. We found that the levels of TC, TG, and LDL-C had decreased ($P < 0.01$), and HDL-C had increased ($P < 0.01$) in both DGSY and X groups. However, the

Table 3 The main chemical components of DGSY

PM	tR/min	Molecular formula	EV	Error(ppm)	Secondary fragment(MS/MS)	compound name
1	0.88	$C_6H_{14}N_4O_2$	174.111970	1.70	158.0、130.10、116.07、70.07、60.06	Arginine
2	0.97	$C_5H_9NO_4$	147.053410	1.70	130.05、102.6、84.05、68.75	Glutamic acid
3	0.98	$C_{12}H_{22}O_{11}$	342.116530	0.94	233.5、191.22、145.0、127.04、85.03	sucrose
4	1.53	$C_9H_{13}N_3O_5$	243.086080	2.29	226.12、198.11、141.05、112.05、70.07	Cytidine
5	1.54	$C_5H_5N_5$	135.054920	3.13	119.04、94.04、70.62	Adenine
6	1.66	$C_6H_5NO_2$	123.032570	4.42	124.04、96.05、80.05	Nicotinic acid
7	2.62	$C_9H_{11}NO_3$	181.074420	2.90	165.06、147.04、136.08、123.04、119.05	L-Tyrosine
8	2.66	$C_6H_{13}NO_2$	131.095110	3.67	118.94、87.10、86.10、69.07	Leucine
9	6.94	$C_9H_{11}NO_2$	165.079530	3.34	149.06、131.05、120.08、103.05	Phenylalanine
10	14.70	$C_{11}H_{12}N_2O_2$	204.090530	3.21	188.07、159.09、146.06、118.07	Tryptophan
11	20.66	$C_9H_6O_3$	162.032170	2.92	145.03、135.04、117.03、107.03、89.04	7-Hydroxycoumarine
12	20.66	$C_{16}H_{18}O_9$	354.095960	2.49	229.91、163.04、145.03、117.03	Chlorogenic acid
13	23.85	$C_{10}H_{11}NO$	161.084570	3.12	144.08、134.10、120.08	3-(2-Hydroxyethyl)indole
14	24.57	$C_{10}H_{12}O_2$	164.084180	2.77	141.06、137.10、105.07、79.06	4-Phenylbutyric acid
15	25.47	$C_{10}H_8O_4$	192.042990	3.79	178.03、165.06、149.06、137.06、133.03	Scopoletin
16	29.08	$C_{12}H_{16}O_4$	224.105390	2.39	207.10、189.09、161.10、119.09、105.07、91.05	Senkyunolide H or Senkyunolide I
17	30.38	$C_{11}H_{14}O_2$	178.099980	3.36	161.10、143.09、133.10、119.09、105.07、91.06	Butyl benzoate
18	30.47	$C_{12}H_{18}O_4$	226.121113	3.07	209.12、191.11、153.06	Senkyunolide J
19	31.04	$C_{11}H_6O_3$	186.032270	3.12	169.07、143.05、131.05、115.05	Psoralen
20	33.99	$C_{15}H_{24}O$	220.183280	2.54	221.19、203.18、163.15、147.12、133.10、107.09	alismol
21	35.98	$C_{12}H_{16}O_2$	192.115570	2.82	175.11、147.12、137.06、91.05	Senkyunolide A
22	37.47	$C_{15}H_{20}O$	216.152113	3.23	199.14、189.16、175.15、145.10、131.08	Atractylon
23	38.11	$C_{12}H_{14}O_2$	190.099810	2.26	191.11、173.10、163.11、145.10、117.07、91.05	Ligustilide
24	38.35	$C_{12}H_{18}O_2$	194.131270	3.06	177.13、149.13、125.06、107.09、97.07、79.06	Sedanolide
25	39.13	$C_{15}H_{26}O_2$	238.193860	2.45	203.18、163.15、147.12、107.09	Alismoxide
26	39.77	$C_{15}H_{20}O_2$	232.146990	2.84	233.15、215.14、187.15、177.09、151.08	Atractylenolide II
27	40.09	$C_{30}H_{46}O_5$	486.336170	3.38	451.32、397.27、353.24、201.13	Alisol C
28	40.50	$C_{32}H_{48}O_6$	528.346783	3.22	469.33、451.32、433.31、381.27、353.25	23-O-Acetylalisol C
29	41.29	$C_{15}H_{18}O_2$	230.131363	2.97	231.13864、185、13	Atractylenolide I
30	41.68	$C_{18}H_{30}O_2$	278.225240	2.36	274.27、226.95、219.18、191.11	Linolenic acid
31	42.11	$C_{16}H_{22}O_4$	278.152450	2.31	149.02、121.10、109.10、95.09、81.07、67.06	Dibutyl phthalate
32	43.25	$C_{32}H_{50}O_5$	514.367300	2.86	478.75、352.08、274.88、201.16、159.12、121.10	23-O-Acetylalisol B
33	43.66	$C_{30}H_{48}O_4$	472.356520	2.68	415.32、348.38、308.74、201.16	Alisol B
34	43.67	$C_{32}H_{48}O_5$	512.349413	-1.49	513.36、449.04、425.97、337.85	Alisol O
35	0.91	$C_4H_7NO_4$	133.037750	1.81	115.00、95.03、88.04、71.01	Aspartic acid
36	0.94	$C_6H_{14}O_6$	182.079360	1.79	163.06、119.04、101.02、96.97、89.02、71.01	Mannitol
37	0.98	$C_6H_{12}O_6$	180.063670	1.58	161.05、131.04、89.02、85.03、71.01、59.01	Fructose
38	1.78	$C_6H_8O_7$	192.027340	1.77	173.26、129.02、111.01、87.01、85.03	Citric acid
39	4.12	$C_6H_6O_3$	126.031880	1.49	107.29、107.29、100.03、97.03	Pyrogallol
40	4.18	$C_7H_6O_5$	170.021517	-0.04	169.01、125.02	Gallic acid
41	4.45	$C_{10}H_{13}N_5O_4$	267.097510	2.83	266.09、134.05、119.04	Adenosine
42	9.63	$C_7H_6O_4$	154.026917	2.00	153.02、109.03	protocatechuic acid
43	16.24	$C_8H_8O_4$	168.042477	1.30	123.05、121.03、101.37、95.05、68.80	Vanillin

Table 3 (continued)

PM	tR/min	Molecular formula	EV	Error(ppm)	Secondary fragment(MS/MS)	compound name
44	16.74	$C_{15}H_{14}O_6$	290.079790	2.59	271.06、203.07、151.04、125.02、109.03	Catechin
45	17.18	$C_{23}H_{28}O_{12}$	496.158067	-0.02	407.66、281.07、165.06、137.02	oxypaeoniflora
46	17.61	$C_{16}H_{18}O_9$	354.095870	2.22	280.83、191.06、179.04、173.05、135.05、93.03	Neochlorogenic acid
47	19.18	$C_8H_8O_3$	152.047640	1.92	136.02、123.05、108.02、95.01	Vanillin
48	20.37	$C_{23}H_{28}O_{11}$	480.164090	1.93	466.12、358.34、327.11、165.06、121.03	albiflorin
49	21.93	$C_{10}H_{10}O_4$	194.058200	1.48	178.03、149.06、137.02、134.04	ferulic acid
50	25.04	$C_9H_{16}O_4$	188.105190	1.77	187.10、169.09、143.11、125.10、97.07	Azelaic acid
51	25.19	$C_{23}H_{28}O_{11}$	480.164320	1.27	433.24、371.50、327.86、221.02、151.08、121.03	Paeoniflorin
52	28.98	$C_{20}H_{20}O_6$	356.126877	2.49	340.10、296.11、281.08、219.07、175.08、147.08	coniferyl ferulate
53	29.30	$C_{15}H_{12}O_5$	272.069170	2.55	271.06、203.07、159.08、130.04	Naringenin
54	34.03	$C_{15}H_{10}O_4$	254.058520	2.39	263.05、209.06、107.01	Chrysin
55	41.54	$C_{31}H_{48}O_4$	484.356427	2.41	483.35、423.33、409.28、310.00、128.12	Dehydrotumulosic acid
56	42.68	$C_{31}H_{46}O_4$	482.340747	2.36	467.71、421.31、403.30、311.20、271.17、97.97	Polyporenic acid C

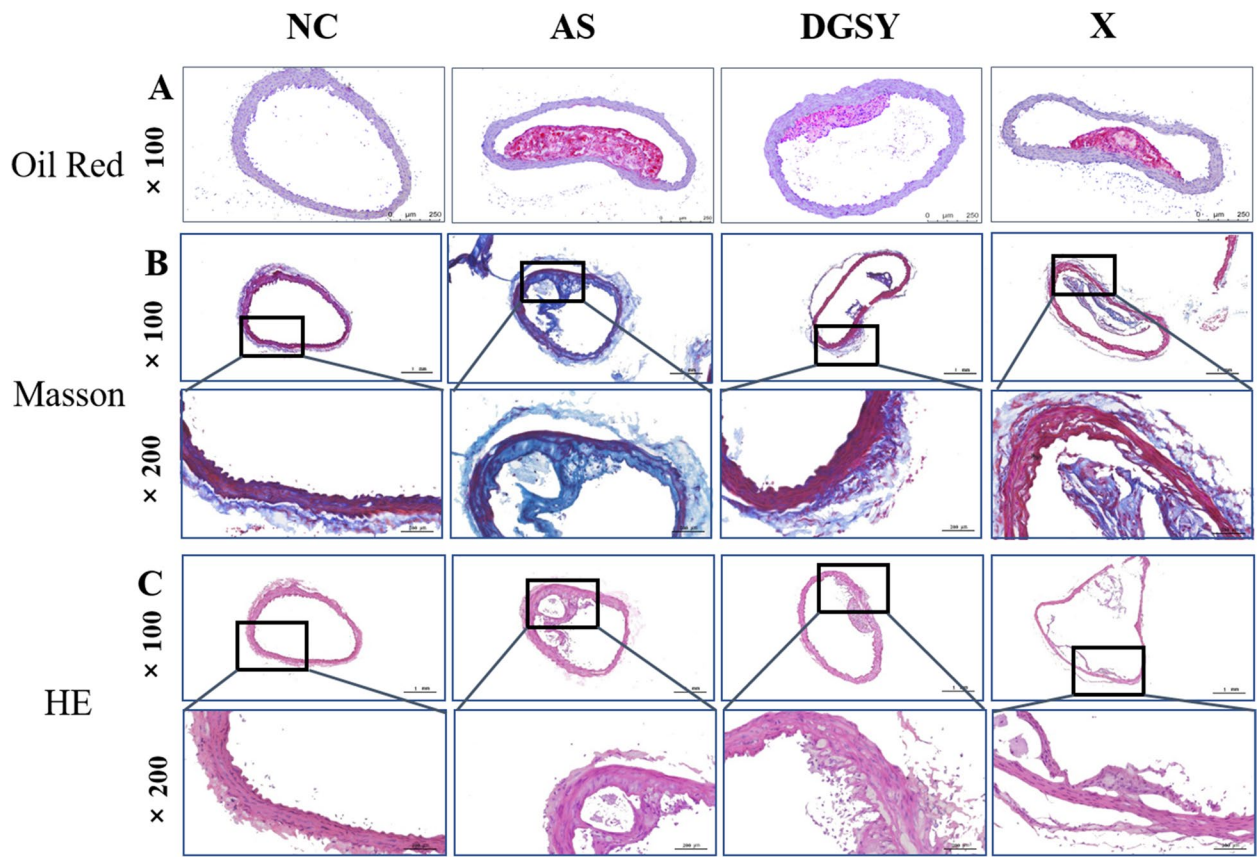

Fig. 2 Effects of DGSY on pathological morphology of aorta in ApoE-/- mice. **A** Oil red staining (× 100), $n = 3$. **B** Masson staining (× 100, × 200), $n = 3$. **C** HE staining (× 100, × 200), $n = 3$

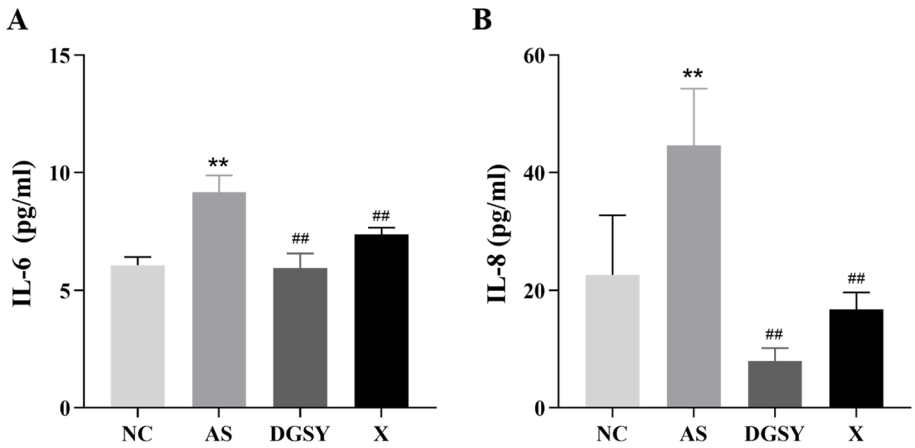

Fig. 4 Effects of DGSY on IL-6 and IL-8 levels. **A** DGSY reduced the level of IL-6. **B** DGSY reduced the level of IL-8. The data are expressed as the means ± S.D. ($n = 6$). $^{**}p < 0.01$ vs NC, $^{\#\#}p < 0.01$ vs AS

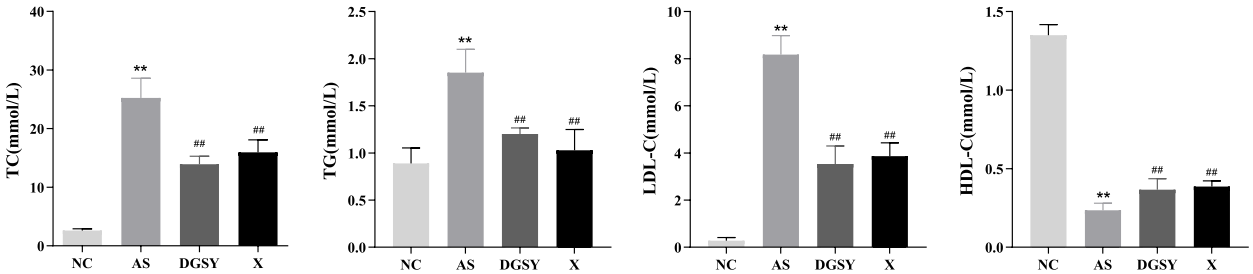

Fig. 3 Effect of DGSY on blood lipid indexes in mice. **A** Changes in the content of TC. **B** Changes in the content of TG. **C** Changes in the content of LDL-C. **D** Changes in the content of HDL-C. The data are expressed as the means ± S.D. ($n = 6$). $^{**}p < 0.01$ vs NC, $^{\#\#}p < 0.01$ vs AS

difference was not significant. Thus, DGSY can improve blood lipid metabolism similar to atorvastatin calcium.

Effects of DGSY on IL-6 and IL-8

Considering that DGSY exerted anti-inflammatory effects, its impact on the levels of IL-6 and IL-8 in vascular tissues was explored with ELISA test. Results shown in Fig. 4 indicated that IL-6 and IL-8 levels were increased in the AS group, and treatment with DGSY and atorvastatin calcium reversed this effect ($P < 0.01$). Importantly, DGYS significantly reduced the levels of IL-6 and IL-8 more than atorvastatin calcium ($P < 0.01$), thus indicating that DGSY is a better relief for vascular endothelial inflammation.

Effects of DGSY on ICAM-1 and VCAM-1

Activation of vascular endothelial cells is the initiating factor of AS. Endothelial cell activation triggers an inflammatory response, which mainly upregulates the expression of adhesion factors ICAM-1 and VCAM-1. Therefore, we measured the expression of VCAM-1 and ICAM-1 by immunohistochemistry (Fig. 5). Concurrently, the semi-quantitative measurement of optical density (IOD) was marked with Image-Pro Plus version 6.0 analysis software to calculate the relative expression of VCAM-1 and ICAM-1. Measure the integral absorbance of the positive expression area in the immunohistochemical sections, and calculate the average absorbance = integral absorbance/aortic cross-sectional area. The average absorbance represented the expression intensity of vascular endothelial adhesion factor in the aorta. In the NC group, the structure of aortic endothelium was clear, and there was almost no expression of VCAM-1 and ICAM-1, as determined from the yellow-stained particles. Brown-yellow particles were significantly less in the aortic endothelium in the DGSY and X groups than in the NC group ($P < 0.01$). This indicates that DGSY and atorvastatin calcium significantly decreased the expression of VCAM-1 and ICAM-1. The decrease in expression was significantly higher in the DGSY than in the X group ($P < 0.01$), indicating that the effects of DGSY were superior to those of atorvastatin calcium.

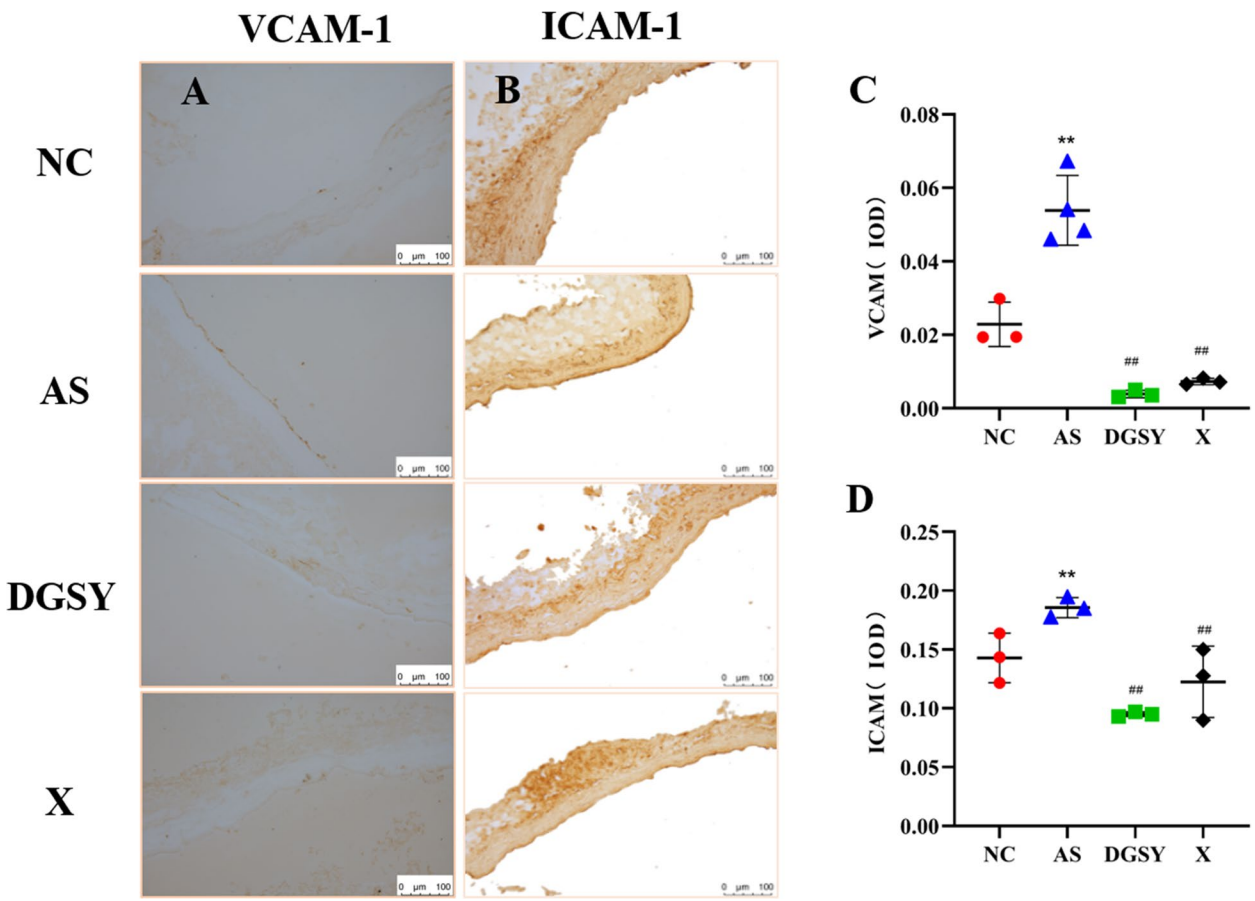

Fig. 5 DGSY inhibited the expression of VCAM-1 and ICAM-1. **A** Expression of VCAM-1 in vascular endothelium (SP, DAB × 200), $n=4$. **B** Expression of ICAM-1 in vascular endothelium (SP, DAB × 200), $n=6$. **C** Bar diagram showing the expression of VCAM-1. **D** Bar diagram showing the expression of ICAM-1. The data are expressed as the means ± S.D. $^{**}p<0.01$ vs, $^{\#\#}p<0.01$ vs AS

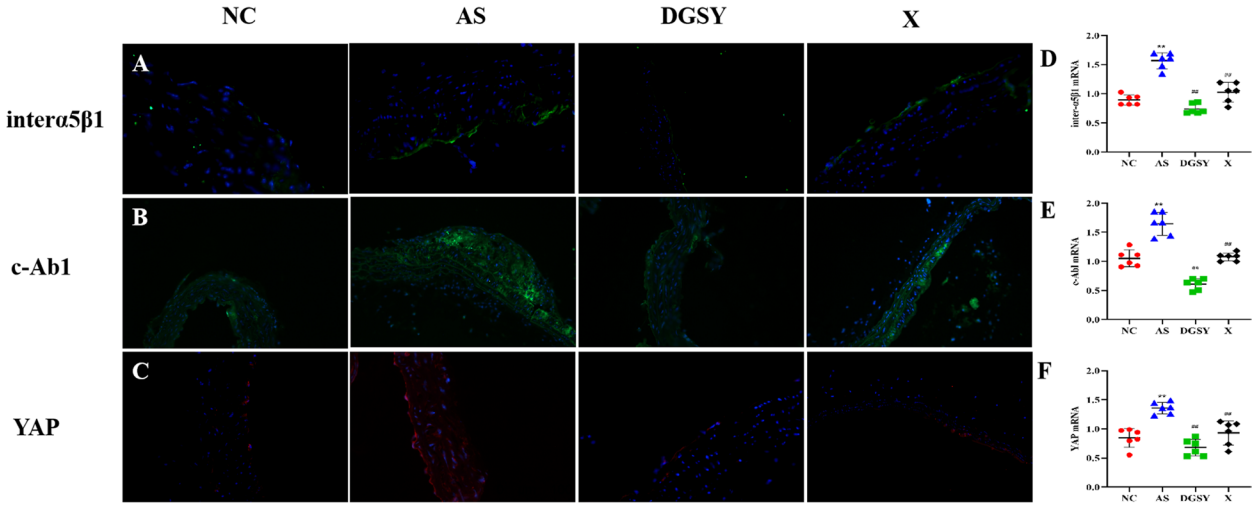

Fig. 6 Effects of DGSY on the levels of inter-α5β1, c-Abl, and YAP in vascular endothelium. **A** Expression of interα5β1 (green) and nuclear (blue), $n=3$. **B** Expression of c-Abl (green) and nuclear (blue), $n=3$. **C** Expression of YAP (red) and nuclear (blue) YAP, $n=3$. **D** The mRNA levels of interα5β1, ($n=6$). (E) The mRNA levels of c-Abl, ($n=6$). (F) The mRNA levels of YAP, ($n=6$). The data are expressed as the means ± S.D. $^{**}p<0.01$ vs, $^{\#\#}p<0.01$ vs AS

Effects of DGSY on interα5β1, c-Abl, and YAP

To determine the effects of DGSY on interα5β1/c-Abl/YAP signal pathways (Fig. 6), their mRNA levels were measured by qT-PCR and the location of expression was assessed by immunofluorescence. The mRNA levels of *interα5β1*, *c-Ab1,* and YAP increased ($P<0.01$) in the AS group, which was consistent with the increased expression from the immunofluorescence assays. The mRNA levels of *interα5β1*, *c-Ab1,* and *YAP* ($P<0.01$) and expression —as assessed by immunofluorescence— were lower in the DGSY and X groups than in the NC group. Levels of interα5β1 and c-Ab1 were lower in DGSY than in the X group ($P<0.01$). However, there was no significant difference between the two groups in YAP expression.

Discussion

Increasing evidence has recently shown that AS is a chronic vascular inflammatory disease. The changes in the structure and function of vascular endothelial cells are the initial steps in the occurrence and development of AS. The vascular endothelium is a multifunctional endocrine organ, which can synthesize and secrete a variety of substances and regulate body processes. The early pathological changes in AS mainly depend on vascular endothelial dysfunction, and this leads to: lipid infiltration; the presence of inflammatory factors, macrophages, and smooth muscle cells accumulation in the blood vessels; damage to the vascular endothelium; loss of vascular wall elasticity; formation of yellow atheroma plaques; and upregulated expression of cell adhesion factor —these suggest that the vascular endothelium plays an important role in the pathogenesis of AS [22–24]. The damage to vascular endothelium can be reversed to some extent [25]. Therefore, protection of the vascular endothelium is an effective way to prevent and treat AS.

DGSY has a protective effect on vascular endothelial cells and plays a protective role in various pathological conditions [26, 27]. However, as with many other traditional Chinese medicines, there are few animal studies on DGSY, most of which are on either a single inflammatory cytokines or vascular adhesion cytokines. To verify the protective effect of DGSY on the vascular endothelium, the levels of blood lipids, inflammatory cytokines, and vascular cell adhesion cytokines were assessed. Moreover, our study determined the turbulence signal of interα5β1 /c-Abl/YAP.

Dyslipidemia is the pathological basis of AS. Increased blood lipid levels can damage vascular endothelial cells, which promotes the release of inflammatory factors that accelerate AS progression [28]. The main components of blood lipids are TC, TG, and LDL-C. Elevated blood lipid levels lead to lipid deposition and free radical release in vascular endothelial and endothelial cells respectively, which exacerbates vascular endothelial dysfunction [29]. Lipids that are predominantly LDL penetrate through vascular endothelial cells into the subcutaneous space where they undergo oxidation to OX-LDL, resulting in cell necrosis that forms atherosclerotic plaques [30]. Relatedly, Austin MA showed that TG —an independent risk factor for atherosclerotic pathogenesis— was associated with vascular endothelial injury [31]. HDL binds excess cholesterol in the body and transports it from the site of plaque damage to the liver, which protects against AS [32]. Therefore, improving lipid metabolism disorders can effectively reduce vascular endothelium damage and prevent AS. This study proved that DGSY significantly reduced TC, TG, and LDL-C ($p<0.01$) and increased HDL-C ($p<0.01$) levels. Interestingly, we found no significant difference in the improvement of blood lipid levels between the DGSY and X groups. Noteworthy was that this effect of DGSY was equivalent to that of atorvastatin calcium.

AS is also hypothesized as a chronic inflammation involving the arterial wall and is closely related to vascular endothelial dysfunction [33]. After arterial vascular damage, many inflammatory cytokines are released and macrophages form foam cells, which activate the NF-κB signaling pathway, which promotes the re-injury of the vascular endothelium. As a result, strips of lipids are easily formed in the vessel wall, causing the vessel to lose its elasticity and form plaques. IL-6 and IL-8 are closely related to vascular endothelial inflammation. QF Zeng demonstrated that IL-6 promoted the expression of LDL receptors in macrophages, enhancing their intake of LDL, thus promoting the formation of foam cells and upregulated expression of adhesion factors and other cytokines [34]. Azghania showed that IL-8 promoted: the accumulation of neutrophils; the tight adhesion of monocytes to endothelial cells; and the invasion of the vascular wall. These aggravated vascular endothelial cell damage [35]. In contrast, macrophages, and damaged endothelial cells release interleukin factors such as IL-6 and IL-8, which exacerbate the inflammatory cascade. Therefore, we evaluated the infiltration of vascular endothelial inflammation by IL-6 and IL-8. DGSY reduced IL-6 and IL-8 levels, suggesting it effectively controlled both the development of inflammation and reduced the inflammatory infiltration of vascular endothelium. Interestingly, DGSY was better in this respect than atorvastatin calcium.

Hemodynamics can affect the function of vascular endothelial cells. Laminar flow and atherosclerotic plaques preferentially develop at branches and curvatures in the arterial system where flow is either turbulent or at low speed [36]. At the cellular and molecular levels, increased abnormal shear stress regulated endothelial inflammation, including the expression of VCAM-1

and ICAM-1. This activated MAPKs, NF-κB, YAP/YAZ, and other signaling pathways to damage vascular endothelial cells [37–40]. VCAM-1 and ICAM-1 promoted the adhesion and migration of inflammatory cells to endothelial cells and the transformation of monocytes to macrophages and foam cells [41]. Conversely, inhibition of VCAM-1 and ICAM-1 reduced endothelial cell activity and attenuated endothelial injury and inflammation [42]. Our study showed that DGSY downregulated the expression of VCAM-1 and ICAM-1, which reduced vascular endothelium damage corroborating previous studies [16]. Moreover, the expression of VCAM-1 and ICAM-1 showed lower for DGSY group than the X group, but there was no great difference in the two groups.

Studies have shown that the interα5β1/c-Abl/YAP signaling pathway is a potential therapeutic target for the treatment of early atherosclerosis [43]. Interα5 and YAP are mechanical force receptors on endothelial cells —interα5 is especially sensitive to shear stress [44]. Turbulence can significantly increase the expression of interα5 in the activated state, triggering proinflammatory responses and proatherogenic phenotypes in vascular endothelial cells. Relatedly, endothelial-specific overexpression of YAP increased the degree of atherosclerosis in mice [45]. As a key upstream factor of turbulence regulation, interα5 can induce YAP to accumulate continuously in the nucleus, upregulate the expression of ICAM-1 and VCAM-1 and promote the proliferation and inflammatory phenotype of endothelial cells.

The c-Abl can activate interα5β1/YAP, and interα5 activation increases c-Abl activity, resulting in phosphorylation of the YAP Y357 residue and subsequent increase in YAP stability [46]. Studies have shown that the inhibitor of c-Abl significantly reduced the phosphorylation of YAP tyrosine 357 following activation by interα5β1. This in turn decreases endothelial inflammation and plaque formation. In our study, the expression of interα5β1,c-Abl, and YAP were used to indicate vascular endothelium damage. Levels of interα5β1/YAP mediated by c-Abl decreased in the vascular tissues of mice in the DGSY group, which was consistent with the immunofluorescence assays, indicating that DGSY significantly alleviated vascular endothelial injury. The reduction of interα5β1,c-Abl, and YAP levels were more obvious in DGSY than in atorvastatin calcium treatment groups, suggesting that DGSY is beneficial for reducing vascular injuries caused by blood flow. Moreover, DGSY improved the function of vascular cells by inhibiting MAPKs and IKK/NF-κB signaling pathways, reducing levels of TNF-α, IL-6, IL-1β, and Cox-2 [47].

Conclusions

In conclusion, our study has demonstrated the potential of DGSY in protecting the vascular endothelium and alleviating AS by modulating expression levels of TC, TG, LDL-C, and HDL-C, reducing IL-6 and IL-8 expression level, inhibiting ICAM-1 and VCAM-1 expression, and suppressing the expression of interα5β1 /c-Abl/YAP signaling pathway. It's worth noting that the effect of DGSY was better than that of atorvastatin calcium which need enlarge the sample size to confirm it in the next step.

Acknowledgements

This study was supported by the National Natural Science Fund Projects and MJ Language Editing Services.

Authors' contributions

YL and LZ: design the study and acquired the funding. YS and YG: supervised the study and wrote the first draft. YL, YZ, and HZ: analyzed the data and processed the images.YT and FZ: Coordinated the study. YS and LZ: critical revision of the manuscript. All authors contributed to the article and approved the submitted version.

Funding

This study was supported by the National Natural Science Fund Projects (Grant no. 82074325).

Availability of data and materials

The datasets presented in the current study are available from the corresponding author upon reasonable request.

Declarations

Ethics approval and consent to participate

All experimental protocols were approved by Animal Ethics Committee, Beijing University of Chinese Medicine (BUCM-4–2021060802-2056). All methods were carried out in accordance with relevant guidelines and regulations and all methods are reported in accordance with ARRIVE guidelines.

Consent for Publication

Not application.

Competing interests

The authors declare no competing interests.

Received: 15 November 2022 Accepted: 11 February 2023
Published online: 20 February 2023

References

1. Soehnlein O, Libby P. Targeting inflammation in atherosclerosis-from experimental insights to the clinic. Nat Rev Drug Discov. 2021;20:589–610. https://doi.org/10.1038/s41573-021-00198-1.
2. Falk E. Pathogenesis of atherosclerosis. J Am Coll Cardiol. 2006;47:C7-12. https://doi.org/10.1016/j.jacc.2005.09.068.
3. Townsend N, Nichols M, Scarborough P, Rayner M. Cardiovascular disease in Europe–epidemiological update 2015. Eur Heart J. 2015;36:2696–705. https://doi.org/10.1093/eurheartj/ehv428.
4. Desjardins F, Balligand JL. Nitric oxide-dependent endothelial function and cardiovascular disease. Acta Clin Belg. 2006;61:326–34. https://doi.org/10.1179/acb.2006.052.
5. Hu S, Gao R, Liu LS, Zhu ML, Wang W, Wang YJ, Wu ZS, Li HJ, Gu DF, Yang YJ, Zheng Z, Chen WW. Summary of China Cardiovascular Disease Report 2018. Chin J Circ. 2019;34:209–20. https://doi.org/10.3969/j.issn.1000-3614.2019.03.001.

6. Chatzizisis YS, Coskun AU, Jonas M, Edelman ER, Feldman CL, Stone PH. Role of endothelial shear stress in the natural history of coronary atherosclerosis and vascular remodeling: molecular, cellular, and vascular behavior. J Am Coll Cardiol. 2007;49:2379–93. https://doi.org/10.1016/j.jacc.2007.02.059. Epub 2007 Jun 8.
7. Zhang K, Chen Y, Zhang T, Huang L, Wang Y, Yin T, Qiu J, Gregersen H, Wang G. A Novel role of id1 in regulating oscillatory shear stress-mediated lipid uptake in endothelial cells. Ann Biomed Eng. 2018;46:849–63. https://doi.org/10.1007/s10439-018-2000-3.
8. Zhang LF. The effects of Danggui Shaoyao San on Atherosclerosis [D]. Hebei Med Univ. 2003. https://doi.org/10.7666/d.y518917.
9. Ren P, Kang QF, Zhou MX, Zhang L, Li SN, Liu WH. Effects of Danggui Shaoyao San on the expression of DNA methyltransferase 1 and PPAR-γin atherosclerotic mice. Glob J Chin Med. 2017;10:1328–32. https://doi.org/10.3969/j.issn.1674-1749.2017.11.009.
10. Liu WH, Jia LC, Zhang L, Kang QF, Zhou MX. Effects of Danggui Shaoyao San serum on inflammatory factors and signaling pathways of RAW 264.7 cells induced by lipopolysaccharide. Glob J Chin Med. 2017;13:1853–8. https://doi.org/10.3969/j.issn.1674-1749.2020.11.005.
11. Jia LC, Zhou MX, Zhang L, Liu WH. Effect of Danggui Shaoyao San on mRNA expression of IL-6, MCP-1, NF-κB and PPARγ in serum of mice with metabolic inflammatory response. J Cap Med Univ. 2014;35:813–7. https://doi.org/10.3969/j.issn.1006-7795.2014.06.025.
12. Wu JH. Effects of Danggui Shaoyao San on blood lipid related indexes in pregnancy-induced hypertension model rats. J Guangxi Univ Tradit Chin Med. 2021;24:52–4. https://doi.org/10.3969/j.issn.2095-6681.2017.35.128.
13. Yan YL, Wang XG, Song XY, Li Q, Chen J, Zhang LF. Angelica extract powder of hyperlipemia rabbit lipid metabolism and hemorheology. J liaoning Tradit Chin Med. 2005;32:170–1. https://doi.org/10.13192/j.l.JTCM2005.02.84.Yanyl.074.
14. Li MM, Xu V, Fu SP, Hou J, Feng Y, Xu ZP, Ni LH, Wang YL, Xuan ZH. Protective mechanism of Danggui Shaoyao powder on podocytes in rats with nephrotic syndrome based on Angii/TRPC6 pathway. Chin JExp Formulas Chin Med. 2021;27:9–18. https://doi.org/10.13422/j.carolcarrollnkisyfjx.20211936.
15. Yan YL, Ji M, Song XY, Li Q, Xu W, Yang XJ. Effects of Danggui Shaoyao Powder on antioxidant capacity and expression of vascular cell adhesion molecule-1 gene in arterial wall of dyslipidemia rats. Chin J Exp Formulas Chin Med. 2007;13:25–8. https://doi.org/10.13422/j.carolcarrollnkisyfjx.2007.02.011.
16. Bi Y, Han X, Lai Y, Fu Y, Li K, Zhang W, Wang Q, Jiang X, Zhou Y, Liang H, Fan H. Systems pharmacological study based on UHPLC-Q-Orbitrap-HRMS, network pharmacology and experimental validation to explore the potential mechanisms of Danggui-Shaoyao-San against atherosclerosis. J Ethnopharmacol. 2021;278:114278. https://doi.org/10.1016/j.jep.2021.114278.
17. Mancini GB, Baker S, Bergeron J, Fitchett D, Frohlich J, Genest J, Gupta M, Hegele RA, Ng D, Pearson GJ, Pope J, Tashakkor AY. Diagnosis, Prevention, and Management of Statin Adverse Effects and Intolerance: Canadian Consensus Working Group Update (2016). Can J Cardiol. 2016;32:S35-65. https://doi.org/10.1016/j.cjca.2016.01.003.
18. Ward NC, Watts GF, Eckel RH. Statin Toxicity. Circ Res. 2019;124:328–50. https://doi.org/10.1161/CIRCRESAHA.118.312782.
19. Zhao Z, Li Y, Zhou L, Zhou X, Xie B, Zhang W, Sun J. Prevention and treatment of COVID-19 using Traditional Chinese Medicine: a review. Phytomedicine. 2021;85:153308. https://doi.org/10.1016/j.phymed.2020.153308.
20. Qi F, Zhao L, Zhou A, Zhang B, Li A, Wang Z, Han J. The advantages of using traditional Chinese medicine as an adjunctive therapy in the whole course of cancer treatment instead of only terminal stage of cancer. Biosci Trends. 2015;9(1):16–34. https://doi.org/10.5582/bst.2015.01019.
21. Wang J, Qi F, Wang Z, Zhang Z, Pan N, Huai L, Qu S, Zhao L. A review of traditional Chinese medicine for treatment of glioblastoma. Biosci Trends. 2020;13(6):476–87. https://doi.org/10.5582/bst.2019.01323.
22. Lusis AJ. Atherosclerosis Nature. 2000;407(6801):233–41. https://doi.org/10.1038/35025203.
23. Roy H, Bhardwaj S, Yla-Herttuala S. Molecular genetics of atherosclerosis. Hum Genet. 2009;125:467–91. https://doi.org/10.1007/s00439-009-0654-5.
24. Nachtigal P, Semecky V, Kopecky M, Gojova A, Solichova D, Zdansky P, Zadak Z. Application of stereological methods for the quantification of VCAM-1 and ICAM-1 expression in early stages of rabbit atherogenesis. Pathol Res Pract. 2004;200:219–29. https://doi.org/10.1016/j.prp.2004.02.008.
25. Lu JX, Guo C, Ou WS, Jing Y, Niu HF, Song P, Li QZ, Liu Z, Xu J, Li P, Zhu ML, Yin YL. Citronellal prevents endothelial dysfunction and atherosclerosis in rats. J Cell Biochem. 2019;120:3790–800. https://doi.org/10.1002/jcb.27660.
26. Li WJ. Protective mechanism of Danggui Shaoyao San on vascular endothelial injury in hyperlipidemia rats. [D]. Hebei College of Traditional Chinese Medicine.2021. https://doi.org/10.27982/d.cnki.ghbyz.2021.000046.
27. Ji M. Experimental study on regulating blood lipid and protecting vascular endothelial cell function of Danggui Shaoyao San (decoction). [D]. Hebei College of Traditional Chinese Medicine. https://doi.org/10.7666/d.y914375.
28. Gimbrone MA Jr, García-Cardeña G. Endothelial Cell Dysfunction and the Pathobiology of Atherosclerosis. Circ Res. 2016;118:620–36. https://doi.org/10.1161/CIRCRESAHA.115.306301.
29 Davignon J, Ganz P. Role of endothelial dysfunction in atherosclerosis. Circulation. 2004;109:II27-32. https://doi.org/10.1161/01.CIR.0000131515.03336.f8.
30. Stocker R, Keaney JF Jr. Role of oxidative modifications in atherosclerosis. Physiol Rev. 2004;84:1381–478. https://doi.org/10.1152/physrev.00047.2003.
31. Austin MA. Epidemiology of hypertriglyceridemia and cardiovascular disease. Am J Cardiol. 1999;83:13F-16F. https://doi.org/10.1016/s0002-9149(99)00209-x.
32. Ross R, Harker L. Hyperlipidemia and atherosclerosis. Science. 1976;193:1094–100. https://doi.org/10.1126/science.822515.
33. Poznyak A, Grechko AV, Poggio P, Myasoedova VA, Alfieri V, Orekhov AN. The Diabetes Mellitus-Atherosclerosis Connection: The Role of Lipid and Glucose Metabolism and Chronic Inflammation. Int J Mol Sci. 2020;21:1835. https://doi.org/10.3390/ijms21051835.
34. Zeng QF, Lu H. Relationship between carotid atherosclerotic plaque and IL-6 and CRP in patients with acute cerebral infarction [J]. Chin J Neurosci. 2016;19:17–9. https://doi.org/10.3969/j.issn.1673-5110.2016.07.010.
35. Azghani AO, Baker JW, Shetty S, Miller EJ, Bhat GJ. Pseudomonas aeruginosa elastase stimulates ERK signaling pathway and enhances IL-8 production by alveolar epithelial cells in culture. Inflamm Res. 2002;51:506–10. https://doi.org/10.1007/pl00012420.
36. Li B, He J, Lv H, Liu Y, Lv X, Zhang C, Zhu Y, Ai D. c-Abl regulates YAPY357 phosphorylation to activate endothelial atherogenic responses to disturbed flow. J Clin Invest. 2019;129:1167–79. https://doi.org/10.1172/JCI122440.
37. Nakayama A, Albarrán-Juárez J, Liang G, Roquid KA, Iring A, Tonack S, Chen M, Müller OJ, Weinstein LS, Offermanns S. Disturbed flow-induced Gs-mediated signaling protects against endothelial inflammation and atherosclerosis. JCI Insight. 2020;5:e140485. https://doi.org/10.1172/jci.insight.140485.
38. Nigro P, Abe J, Berk BC. Flow shear stress and atherosclerosis: a matter of site specificity. Antioxid Redox Signal. 2011;15(5):1405–14. https://doi.org/10.1089/ars.2010.3679.
39. Zhou J, Li YS, Chien S. Shear stress-initiated signaling and its regulation of endothelial function. Arterioscler Thromb Vasc Biol. 2014;34:2191–8. https://doi.org/10.1161/ATVBAHA.114.303422.
40. Humphrey JD, Dufresne ER, Schwartz MA. Mechanotransduction and extracellular matrix homeostasis. Nat Rev Mol Cell Biol. 2014;15:802–12. https://doi.org/10.1038/nrm3896.
41. Xue F, Yuan HG, Zhao G. Effects of decoction of Salicaria japonicum on the expression of NF-κB in aorta and serum ICAM-1, VCAM-1 and P-seletin in AS rats [J]. J Liaoning Univ Tradit Chin Med. 2016;18:31–4. https://doi.org/10.13194/j.iSSN.1673-842-x.2016.10.009.
42. Rijcken E, Krieglstein CF, Anthoni C, Laukoetter MG, Mennigen R, Spiegel HU, Senninger N, Bennett CF, Schuermann G. ICAM-1 and VCAM-1 antisense oligonucleotides attenuate in vivo leucocyte adherence and inflammation in rat inflammatory bowel disease. Gut. 2002;51:529–35. https://doi.org/10.1136/gut.51.4.529.
43. Li BC. Role and mechanism of Hippo-YAP pathway in turbulence induced vascular endothelial activation and atherosclerosis [D]. Tianjin Medical University,2018.
44. Tzima E, del Pozo MA, Shattil SJ, Chien S, Schwartz MA. Activation of integrins in endothelial cells by fluid shear stress mediates Rho-dependent cytoskeletal alignment. EMBO J. 2001;20:4639–47. https://doi.org/10.1093/emboj/20.17.4639.

45. Wang KC, Yeh YT, Nguyen P, Limqueco E, Lopez J, Thorossian S, Guan KL, Li YJ, Chien S. Flow-dependent YAP/TAZ activities regulate endothelial phenotypes and atherosclerosis. Proc Natl Acad Sci U S A. 2016;113:11525–30. https://doi.org/10.1073/pnas.1613121113.
46. Meng F, Zhou R, Wu S, Zhang Q, Jin Q, Zhou Y, Plouffe SW, Liu S, Song H, Xia Z, Zhao B, Ye S, Feng XH, Guan KL, Zou J, Xu P. Mst1 shuts off cytosolic antiviral defense through IRF3 phosphorylation. Genes Dev. 2016;30:1086–100. https://doi.org/10.1101/gad.277533.116.
47. Fu X, Wang Q, Wang Z, Kuang H, Jiang P. Danggui-Shaoyao-San: new hope for Alzheimer's disease. Aging Dis. 2016;7:502–13. https://doi.org/10.14336/AD.2015.1220.

Publisher's Note